# Miniature Modular Sensor for Chemical Species Tomography with Enhanced Spatial Resolution in Laser Absorption Spectroscopy Tomography

Rui Zhang, Jiangnan Xia, Hugh McCann, Chang Liu
*School of Engineering*
*University of Edinbutgh*
Edinburgh, UK
C.Liu@ed.ac.uk

Ihab Ahmed, Mohamed Pourkashanian
*Department of Mechanical Engineering*
*University of Sheffield*
Sheffield, UK

Andrew Gough, Ian Armstrong, Michael Lengden, Walter Johnstone
*Department of Electronic and Electrical Engineering*
*University of Strathclyde*
Glasgow, UK

*Abstract*— To characterize low/zero-carbon combustion processes, there is a growing demand for imaging of physiochemical parameters with enhanced spatial resolution. Chemical Species Tomography (CST), utilizing multiple line-of-sight Laser Absorption Spectroscopy (LAS) measurements, has gained popularity in industrial applications due to its non-intrusive nature, robustness, and high sensitivity. Typically, existing CST sensors have few centimeters beam spacing and are highly customized for specific applications. To enhance the spatial resolution as well as improving the reconfiguration of the CST sensors, this paper proposes a miniature modular CST sensor with a 1cm beam spacing. The use of off-the-shelf components significantly reduces the cost of the system, making it more practical for industrial implementation. Experimental evaluation of the prototype sensor has been conducted for measurements of temperature and water vapor concentration. The results show consistent and accurate measurements, indicating good reliability of the sensor. The proposed miniature modular sensor offers increased flexibility and adaptability to the various CST systems, paving the way for its commercialization in industrial settings.

*Keywords—Miniature sensor, laser absorption spectroscopy, chemical species tomography*

## I. INTRODUCTION

To inform new understanding and modelling of the next-generation low/zero-carbon combustion systems, temperature and post-combustion species concentration are timely needed to be measured to reflect the combustion instability and efficiency [1]. To date, measurements of temperature and species concentration of industrial flames mainly rely on thermocouples and gas analysers, respectively. However, they can only provide a slow temporal response, e.g., at second level with pointwise measurement. A lack of rapid and accurate *in situ* sensors hinders the characterisation of the dynamic combustion processes.

Chemical species tomography (CST) has gained significant attention in industry due to its non-intrusive nature, robustness, and high sensitivity [2] In various applications, there is a growing need for highly spatially resolved CST measurements to obtain detailed structural information that can enhance combustion diagnosis [3]. However, practical implementation of CST is challenged due to limited optical access, particularly in terms of beam arrangement and system hardware. Among different beam arrangement schemes, the parallel beam arrangement has received considerable attention due to its advantages, including isolated beam paths and uniform sampling throughout the sensing region [4].

A few existing CST systems have been applied for industrial measurements. For instance, P. Wright et al. [5] demonstrated a system with 32 parallel beams in 4 equiangular projections of 8 beams for hydrocarbon vapor imaging in a premix chamber of a multi-cylinder automotive engine. They achieved a temporal resolution of 8 kHz with dual-wavelength measurement. Similarly, L. Ma et al. [6]. developed a fast parallel LAS sensor system for measuring exhaust temperature and water vapor in an aero-propulsion engine (General Electric J85) at a rate of 50 kHz. Their system employed 30 orthogonal beams distributed in the sensing region, and three laser frequencies were combined using Time Division Multiplexing (TDM). These examples highlight the capability of CST sensors in industrial environments for rapid and reliable combustion analysis.

However, to improve the spatial resolution by densely sampling the sensing region , a compact sensor system with 24 channels and an approximate 1 cm beam spacing was designed by F. Wang et al. [7]. This design overcomes the limitations of larger beam spacing found in typical systems, which are often on the scale of a few centimetres. Lab tests conducted on a flat flame burner demonstrated the system's capability to reconstruct temperature distributions in various shapes. Subsequent reports on parallel systems have not shown significant reductions in beam spacing due to the limitations in fibre and component packaging size. Furthermore, most existing implementations are highly specialized and tailored to specific applications. Significant costs have been incurred for customizing the optical mechanics, which hinders commercialization of the CST sensors for various combustion systems.

This paper presents a novel approach to enhance the spatial resolution of CST sensors and improve their versatility with reconfigurable optical layout. It proposes a miniature modular design for both the emitter and receiving sensor, allowing for a 1cm beam spacing. The key contributions can be summarized as follows:

1. Flexibility: The miniaturized and modular design increases the system's flexibility, enabling its utilization in various research and application scenarios.

2. Robustness: The modular design facilitates easy transportation, assembly, maintenance, and replacement of the tomography system, making it well-suited for challenging environments.

3. Cost-effectiveness: By utilizing off-the-shelf components, the sensor's cost is significantly reduced, enhancing its practicality and accessibility.

Miniature modular sensor for chemical species tomography with enhanced spatial resolution

## II. METHODOLOGY

### A. Fundimentals of LAS

The fundamentals of LAS and the noise resistance Wavenumber Modulation Spectroscopy (WMS) have been detailed in previous literatures [8-10], a brief review is provided here for convenience.

When the incident laser beam passes through the target absorbing gas species and is received by a photodetector, the transmitted laser intensity $I_t$ can be described using the Beer-Lambert law:

$$I_t(t) = I_0(t)\exp[-A\phi(v(t),T,P,\chi)]. \qquad (1)$$

where $\phi$ is the lineshape of the spectral absorption feature, which is a function of $v(t)$, temperature $T$ [K], the partial pressure of the absorbing species $P$ [atm], and gas mole fraction $\chi$. $A$ is the path-integrated absorption:

$$A = \int_0^L S(T)P\chi dl, \qquad (2)$$

where $S(T)$ [cm$^{-2}$atm$^{-1}$] is the temperature-dependent linestrength and $L$ [cm] the absorbing path length.

In the WMS technique, the driving current of the laser diode that is consist of a high-frequency sinusoidal modulation $f_m$ [Hz] with a low-frequency sinusoidal scan $f_s$ [Hz]. resulting in the laser's output intensity and frequency being modulated. The interaction of the wavenumber modulated incident light intensity signals, $I_0(t)$, with the absorbing gas results in the $I_t(t)$, that can be described as a Fourier series of terms at the harmonics of the high frequency sinusoidal modulation. With the harmonics containing the absorption information, the path-integrated absorption $A$ can be extracted via spectral fitting [11].

Two path-integrated absorption values, $A_1$ and $A_2$, can be obtained through WMS using two spectral features of the same gas species, and their ratio, $R(T)$, is utilized to calculate the temperature along the path of the light using the following equation [12]:

$$R(T) = \frac{S_2(T)\chi L}{S_1(T)\chi L} = \frac{S_2(T)}{S_1(T)}, \qquad (3)$$

### B. CST sensor archtecture

A CST system designed for simultaneous temperature and species concentration measurements typically consists of four main components: the laser driving system, optical distribution system, optical detection system, and data acquisition system. The laser driving system receives control signals from a workstation or PC and generates different driving currents for the lasers. These driving signals are typically modulated at different frequencies to enable frequency division multiplexing (FDM) for simultaneous detection of two absorption features [13] The laser signals then pass through the optical distribution system, which couples and splits the light intensity signals according to the desired distribution pattern, and emits them into the detection area. The transmitted light is collected by detectors, which convert the light intensity signals into voltage signals. These voltage signals are then acquired by the data acquisition (DAQ) system [14]and sent to the workstation for subsequent data post-processing.

Figure 1 illustrates an octagonal tomographic imaging system with 128 channels, where the laser beams are projected from four directions, with each direction having 32 channels of signals. Typically, the central area with the densest rays is defined as the area of interest (RoI), which covers the detection. The number of rays and their spacing directly influence the number of physical information samples within the RoI [4] Therefore, miniaturization of the transmitter and receiver components in the system plays a crucial role in increasing the number of samples and improving the spatial resolution of the detection process.

## III. SENSOR CONFIGERATION

### A. Emitter

As shown in Fig.2 (a), The emitter with a dimension of 30 mm × 30 mm × 9 mm is mainly composed of three parts: the collimator, the adjusting mirror, and the supporting frame.

To compensate for the large divergence angle of the laser emitted from the optical fibre, a collimator is necessary to collimate the laser beam and ensure adequate light intensity can be revived after propagating the detection path. Among various options for collimation, a C-lens is preferred over grin lens and ball lens for several reasons. Firstly, it offers cost-effectiveness, making it a more affordable choice. Secondly, it provides a wide frequency coverage, allowing it to be used with a range of laser wavelengths. Lastly, it offers a long working distance, enabling effective collimation over larger distances.

Instead of directly aligning the collimator with the detection path, an alternative approach is employed, where the
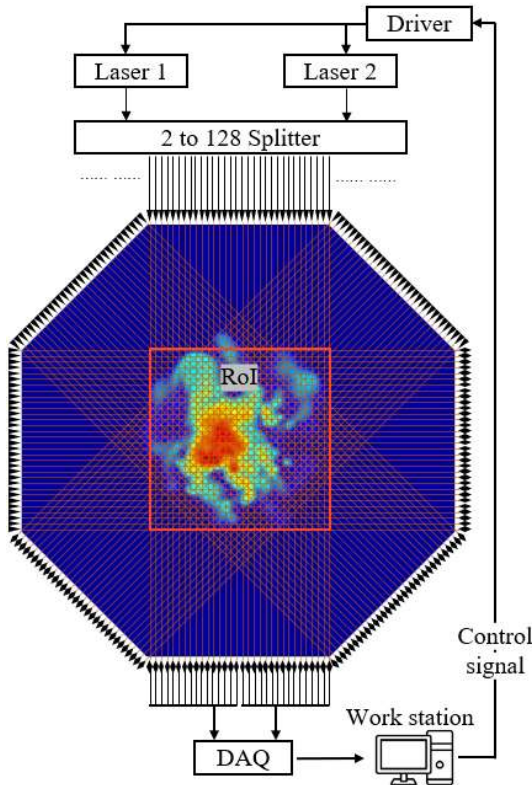


Fig.1 Schematic diagram of an exampled 128-channel CST system.

collimator is positioned perpendicular to the optical path. In this configuration, a right-angle prism is utilized to redirect the collimated laser beam towards the desired detection path. A customized fixing mechanism is employed to securely hold the right-angle prism in place. This fixing mechanism is connected to the supporting frame through the use of a spring, which provides stability and allows for flexibility in the system. Additionally, three screws are utilized to introduce extension of the spring and adjust the position of the mirror, enabling precise alignment and fine-tuning of the laser beam direction. By adjusting the screws, two-dimensional laser beam alignment can be achieved. Taking into consideration the distance between the reflective mirror and the 4mm aperture on the supporting frame, the collimated laser beam at the emitting side can be adjusted within a range of 5 degrees.

In practical applications, due to tolerance, it is still necessary to measure the size of the laser spot on the working
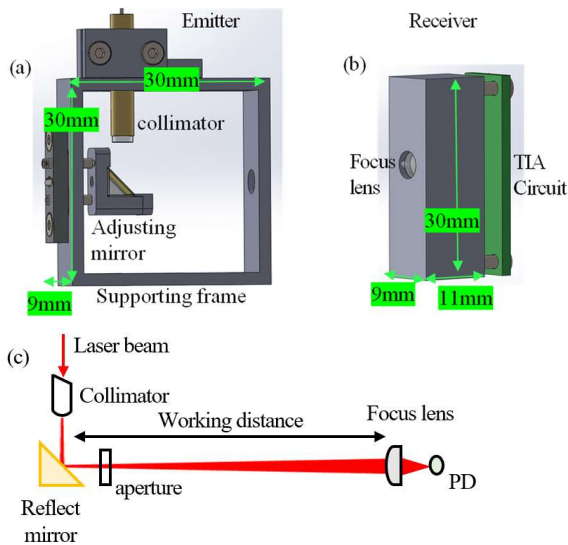


Fig. 2 Diagram of the (a) emitter, (b) receiver and (c) light path of the modular sensor design.
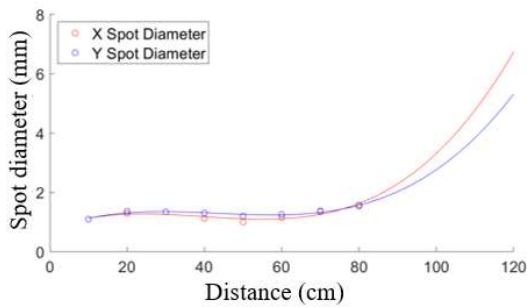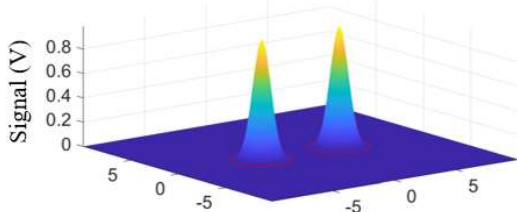


Fig. 3 Characterization of the laser beam spot size and cross talk check for two adjacent laser beams.

distance, ensuring sufficient light intensity emitted to the receiving end. This can be achieved using a beam profiler. The test results are presented in Fig. 3.

*B. Receiver*

An InGaAs PIN photodiode (PD) with a TO-18 cap from Hamamatsu is utilized to collect the transmitted light signal. To convert the current generated by the photodiode into voltage and amplify it to a suitable level for the DAQ, a customised Trans-impedance Amplifier (TIA) was designed using AD8066 (Analog Devices). By considering the linearity of the photodiode, voltage gain and detector bandwidth, a voltage gain of 2k is chosen for the detector. This configuration allows for an output voltage signal of ~1 V when receiving a 0.5 mW light signal. Additionally, the detector's bandwidth is sufficient to accommodate a modulation frequency of up to 200 kHz, which is suitable for WMS implemented in this work. The frequency response of the detector is simulated using Multisim software, and gives a $f_{3dB} \approx 8MHz$. The results are illustrated in Fig. 4.

As shown in Fig.2 (b), to ensure maximum reception of the laser beam by the PD in the presence of device tolerance and beam steering during engine combustion, a plano-convex mirror is employed in front of the PD. This mirror serves to focus the laser beam onto the small photosensitive surface (1 mm) of the PD. The PD target surface is positioned at the focal length of the plano-convex mirror, enabling optimal laser reception.

YG2021QN37.A validation test was performed to compare the measurement results of room temperature and ambient water concentration obtained from three adjacent channels of the modular prototype, as depicted in Fig.5, with the readings of a humidity sensor (Sensirion, SHT31). Both two kinds of sensors and the gas path for detection are sealed in a box to mitigate interference. In terms of the laser driving of the prototype sensor, two distributed-feedback (DFB) laser diodes (NEL NLK1E5EAAA and NEL NLK1B5EAAA) are used to generate lasers at 7185 $cm^{-1}$ and 7444 $cm^{-1}$, respectively for simultaneous temperature and water concentration measurement by implementing FDM [13]. Both
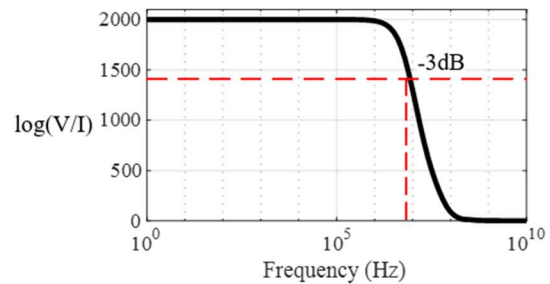


Fig. 4 Frequency response of the TIA with a gain of 2k.
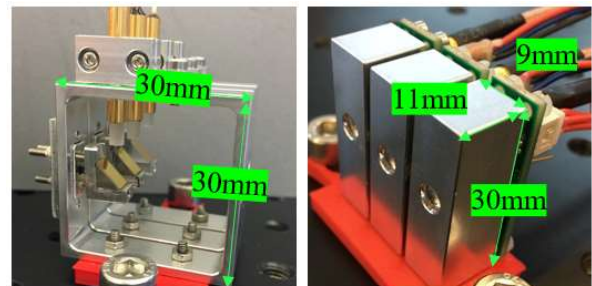


Fig. 5 Three channel of the modular LAS sensors prototyped for the test.

lasers were scanned by 1 kHz sinusoid and modulated with 100 kHz and 130 kHz sinusoid, respectively. This enables a temporal resolution of 1 kHz. A continuous measurement of the temperature and water concentration was carried out for 5 minutes. The light was coupled and split into 4 channel, three of the four are connected to the emitters. The detected signals are then digitized by a Red Pitaya (RP)-based DAQ system [14] and sent to the desktop for post-processing. The measurement results was given by Table I.

Overall, the three sensors showed similar test results, but the LAS sensors recorded slightly higher water concentration measurements compared to the humidity sensor. The fluctuations in water concentration over a 5-minute period were approximately 4.2%. On the other hand, the LAS sensors consistently provided lower temperature measurements compared to the reference values. The temperature fluctuations are also twice as high as the concentration measurements. This difference can be attributed to the weaker linestrength at 7444 cm$^{-1}$ at room temperature, which is only one-fifth of that at 7185 cm$^{-1}$. Additionally, when calculating the temperature ratio, the inclusion of the 7444 cm$^{-1}$ line introduces its own fluctuations into the computation, resulting in an overall lower calculated temperature value. It is worth noting that temperature measurements are more susceptible to noise interference in this setup.

To analyse the noise in the measurements, an Allan deviation analysis was conducted to assess the stability of the H2O measurement. As depicted in Figure 6, the three measurements overlap with each other and closely follow the $1/\sqrt{\tau}$ trend. This indicates that the three sensors exhibit similar noise performance and that their measurements are primarily influenced by white noise.

TABLE I. COMPARE THE TEST RESULTS OF TEMPERATURE AND H$_2$O CONCENTRATION FROM THERR SENSOR PROTOTYPES WITH HUMIDITY SENSOR

| Metrics / Sensors | H$_2$O concentration | | Temperature (°C) | |
|---|---|---|---|---|
| | Mean | STD | Mean | STD |
| SHT31 (Reference) | 0.0079 | \ | 21.89 | \ |
| Channel1 | 0.0082 | 4.2% | 20.32 | 8.1% |
| Channel2 | 0.0082 | 4.0% | 20.35 | 7.6% |
| Channel3 | 0.0081 | 4.5% | 20.39 | 8.1% |
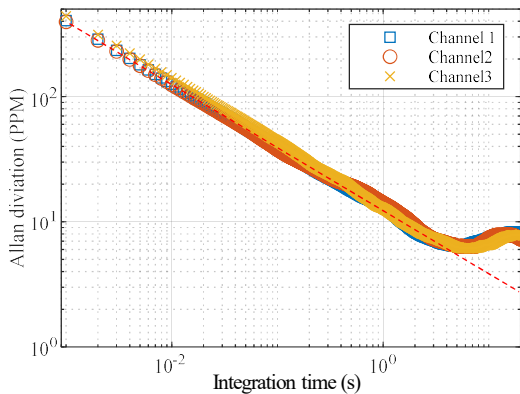


Fig. 6 Allan deviation analysis at 1 atm and room temperature. The dash red line proportional to $\sqrt{\tau}$ indicates the theoretically expected behaviour of the system dominated by white noise.

## IV. CONCLUSION

This paper introduces a miniature modular sensor design for CST imaging with enhanced spatial resolution. The design focuses on reducing the size of both the emitter and receiver components, resulting in dimensions of 30 mm × 30 mm × 9 mm and 11 mm × 30 mm × 9 mm, respectively. This compact design allows for a flexible beam arrangement with a beam spacing of 1 cm and a temporal resolution of 1 kHz in the CST system. A prototype of the sensor has been fabricated and tested in laboratory conditions. The sensor's performance was evaluated by measuring room temperature and ambient water concentration, and the obtained results were compared to reference measurements. The experimental results show that the measurements using the developed sensor closely align with the reference values, with a 4% fluctuation observed due to the presence of white noise. This demonstrates the good reliability and accuracy of the proposed sensor design.

## REFERENCES

[1] D. Burnes and A. Camou, "Impact of fuel composition on gas turbine engine performance," *Journal of Engineering for Gas Turbines and Power,* vol. 141, no. 10, p. 101006, 2019.

[2] H. McCann, P. Wright, K. Daun, S. J. Grauer, C. Liu, and S. Wagner, "Chemical species tomography," in *Industrial Tomography*: Elsevier, 2022, pp. 155-205.

[3] B. Fu et al., "Recent progress on laser absorption spectroscopy for determination of gaseous chemical species," *Applied Spectroscopy Reviews*, vol. 57, no. 2, pp. 112-152, 2022.G.

[4] C. Liu, S.-A. Tsekenis, N. Polydorides, and H. McCann, "Toward customized spatial resolution in TDLAS tomography," *IEEE Sensors Journal*, vol. 19, no. 5, pp. 1748-1755, 2018.

[5] P. Wright *et al.*, "Toward in-cylinder absorption tomography in a production engine," *Applied optics,* vol. 44, no. 31, pp. 6578-6592, 2005.

[6] L. Ma *et al.*, "50-kHz-rate 2D imaging of temperature and H 2 O concentration at the exhaust plane of a J85 engine using hyperspectral tomography," *Optics express,* vol. 21, no. 1, pp. 1152-1162, 2013.

[7] F. Wang, Q. Wu, Q. Huang, H. Zhang, J. Yan, and K. Cen, "Simultaneous measurement of 2-dimensional H2O concentration and temperature distribution in premixed methane/air flame using TDLAS-based tomography technology," *Optics Communications,* vol. 346, pp. 53-63, 2015.

[8] A. Farooq, A. B. Alquaity, M. Raza, E. F. Nasir, S. Yao, and W. Ren, "Laser sensors for energy systems and process industries: Perspectives and directions," *Progress in Energy and Combustion Science,* vol. 91, p. 100997, 2022.

[9] C. S. Goldenstein, R. M. Spearrin, J. B. Jeffries, and R. K. Hanson, "Infrared laser-absorption sensing for combustion gases," *Progress in Energy and Combustion Science,* vol. 60, pp. 132-176, 2017.

[10] C. Liu and L. Xu, "Laser absorption spectroscopy for combustion diagnosis in reactive flows: A review," *Applied Spectroscopy Reviews,* vol. 54, no. 1, pp. 1-44, 2019.

[11] C. S. Goldenstein, C. L. Strand, I. A. Schultz, K. Sun, J. B. Jeffries, and R. K. Hanson, "Fitting of calibration-free scanned-wavelength-modulation spectroscopy spectra for determination of gas properties and absorption lineshapes," *Applied optics,* vol. 53, no. 3, pp. 356-367, 2014.

[12] C. S. Goldenstein, I. A. Schultz, J. B. Jeffries, and R. K. Hanson, "Two-color absorption spectroscopy strategy for measuring the column density and path average temperature of the absorbing species in nonuniform gases," *Applied optics,* vol. 52, no. 33, pp. 7950-7962, 2013.

[13] A. Huang, Z. Cao, W. Zhao, H. Zhang, and L. Xu, "Frequency-division multiplexing and main peak scanning WMS method for TDLAS tomography in flame monitoring," *IEEE Transactions on*

*Instrumentation and Measurement,* vol. 69, no. 11, pp. 9087-9096, 2020.

[14] G. Enemali, R. Zhang, H. McCann, and C. Liu, "Cost-effective quasi-parallel sensing instrumentation for industrial chemical species tomography," *IEEE Transactions on Industrial Electronics,* vol. 69, no. 2, pp. 2107-2116, 2021.